Direct Measurements of Reynolds Stresses and Turbulence in the Bottom Boundary Layer

Joseph Katz
Department of Mechanical Engineering, and
Center for Environmental and Applied Fluid Mechanics
Johns Hopkins University, 3400 N. Charles Street
Baltimore, MD 21218
phone: (410) 516-5470 fax: (410) 516-7254 email: katz@titan.me.jhu.edu

Thomas Osborn
Department of Earth and Planetary Sciences, and
Center for Environmental and Applied Fluid Mechanics
The Johns Hopkins University
3400 N Charles Street
Baltimore, MD 21218-2681
phone (410) 516-7039   fax (410) 516-7933 email osborn@jhu.edu

LONG-TERM GOALS

a. Measure the Reynolds stresses, velocity profile, vorticity distribution and transport, dissipation rate, and turbulent spectra in the bottom boundary layer of the coastal ocean using Particle Image Velocimetry (PIV). The objective is to obtain data that is free of wave contamination.

b. Quantify the temporal variation of turbulent stresses, turbulence production, dissipation and spectra in relation to the oceanographic parameters that represent the local environment, such as waves, currents, vertical density gradient, internal waves and the nature of the water-sediment interface. The conclusions will quantify the relative importance of different mechanisms that control the flow and turbulence in the benthic boundary layer.

c. Study the mechanisms and extent of sediment re-suspension process, while measuring the details of the evolving flow structure causing this entrainment. The data will enable us to determine whether sediment re-suspension is caused by large scale eddies, as small scale laboratory studies and atmospheric boundary layer data seem to indicate, shear caused by the mean flow over the bottom, or interaction of mean flow with ripples or other bottom features.

d. Use oceanic PIV data for addressing Sub-Grid Scale Modeling issues for Large Eddy Simulation.

e. Examine the structure of the flow, vertical vorticity transport, formation and upward migrations of large coherent vortex structures. Presently there is very little information on the dynamics and impact of large coherent structure in the bottom boundary layer on turbulence and sediment entrainment.

1. REPORT DATE **30 SEP 2001**	2. REPORT TYPE	3. DATES COVERED **00-00-2001 to 00-00-2001**
4. TITLE AND SUBTITLE **Direct Measurements of Reynolds Stresses and Turbulence in the Bottom Boundary Layer**		5a. CONTRACT NUMBER
		5b. GRANT NUMBER
		5c. PROGRAM ELEMENT NUMBER
6. AUTHOR(S)		5d. PROJECT NUMBER
		5e. TASK NUMBER
		5f. WORK UNIT NUMBER
7. PERFORMING ORGANIZATION NAME(S) AND ADDRESS(ES) **Department of Mechanical Engineering, and,Center for Environmental and Applied Fluid Mechanics,,Johns Hopkins University, 3400 N. Charles Street,,Baltimore,,MD, 21218**		8. PERFORMING ORGANIZATION REPORT NUMBER
9. SPONSORING/MONITORING AGENCY NAME(S) AND ADDRESS(ES)		10. SPONSOR/MONITOR'S ACRONYM(S)
		11. SPONSOR/MONITOR'S REPORT NUMBER(S)
12. DISTRIBUTION/AVAILABILITY STATEMENT **Approved for public release; distribution unlimited**		
13. SUPPLEMENTARY NOTES		
14. ABSTRACT		
15. SUBJECT TERMS		

16. SECURITY CLASSIFICATION OF:			17. LIMITATION OF ABSTRACT **Same as Report (SAR)**	18. NUMBER OF PAGES **11**	19a. NAME OF RESPONSIBLE PERSON
a. REPORT **unclassified**	b. ABSTRACT **unclassified**	c. THIS PAGE **unclassified**			

OBJECTIVES

Our effort for the past year focused on several objectives:

a. Analysis of PIV data that was obtained in a previous deployment, mostly a data set obtained near LEO–15 during summer 2000. In these experiments we recorded data in two sample areas simultaneously (details follow). Overcoming the effect of wave contamination of turbulence data in order to calculate the Reynolds stresses has been a major issue.

b. Two field trips (funded in part by the present ONR grant and in part by NSF) to the vicinity of LEO-15 took place this year. In the first we have tested a new platform that extends our profiling range from 1.4m to 9.75m above the bottom. This system is described in the following section. During the second trip we deployed the new platform and obtained an extensive data base, some in the bottom boundary layer, and some in the water column above it. Data analysis is in progress.

APPROACH

Particle image velocimetry (PIV) is capable of mapping two components of the instantaneous velocity distribution within an entire section of a flow field. Our original submersible PIV system described in Bertuccioli et al. (1999) and Doron et al. (2001) has been greatly improved. The present image acquisition system consists of two digital cameras operating simultaneously, each with a sample area of up to $0.5 \times 0.5 \ m^2$. Separation between waves and turbulence while computing the Reynolds stresses in environments with mean flow and waves is performed using an approach introduced by Trowbridge (1998). The data discussed in this report was obtained near LEO-15. Development of a new profiling platform (funded in part by NSF) now enables us to extend our range of measurements from the bottom into the water column up to 9.75m above the bottom. The elevation is controlled by a rugged hydraulic telescopic arm, and a turn-table enables us to align the laser sheets with the flow direction. Deployments tests of the new platforms have already been performed and a series of successful experiments have already taken took in early September 2001.

WORK COMPLETED

Based on the experience gained with the original oceanic PIV system, we constructed and deployed a substantially enhanced PIV system. Figure 1 shows the submersible platform (as it was deployed until last year - the new platform that uses the same optics is described later). Components located on the boat are sketched in Figure 2. The system enables us to simultaneously operate two 2048x2048 pixels, 4 frames/s, high sensitivity, 12 bit digital cameras with custom made hardware-based image shifters to overcome directional ambiguity. When these cameras record double-exposure images the two overlapping frames are shifted on the CCD array relative to each other by a prescribed number of pixels. The magnitude of the shift can be adjusted to be larger than all possible displacements in a certain direction. Consequently, all the particle traces appear to be moving in the same direction and the known fixed displacement is subtracted after processing the images.

Due to the resolution and sensitivity of these cameras, it is possible to sample up to $0.5 \times 0.5 \ m^2$ without compromising the smallest scales (0.6-0.8 cm). Each camera feeds data to a high-speed disk array with a capacity of 240 GB that can acquire data at a sustained maximum acquisition rate of 60 MB/s. Only 32 MB/s are needed for the present system but it can support also the 7.5 image pair/s, 2kx2k cross-correlation cameras that we may use in future tests. The data is compressed without loss of resolution and then backed-up on another hard disk and tapes. The storage capacity of this new system enables us
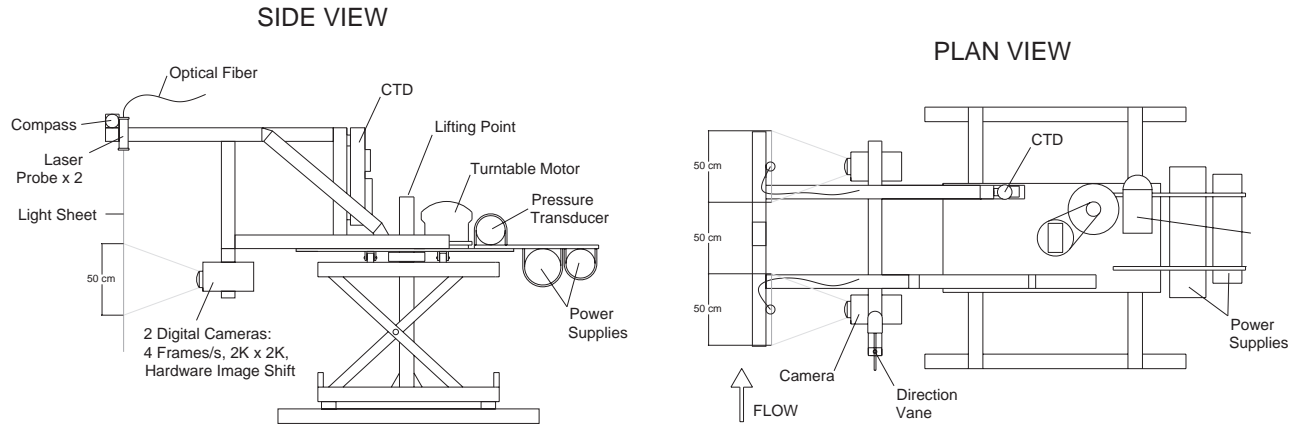
SIDE VIEW

PLAN VIEW

Figure 1: The submersible PIV system during the deployment near LEO 15, May 8-20, 2000. This platform has a maximum profiling range of 1.8 m. A motorized drive rotates the platform to align the sample area with the mean flow direction.
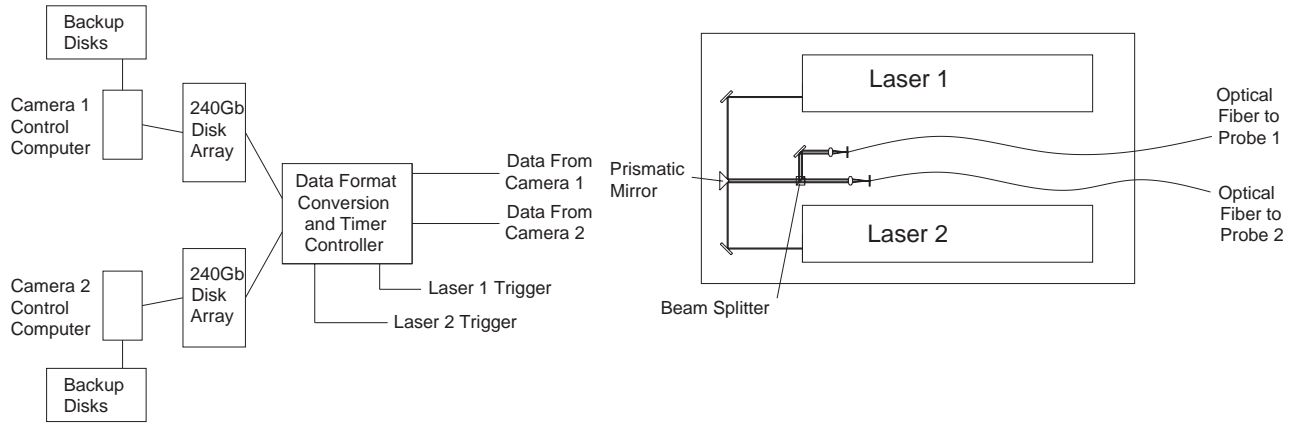

Figure 2: The surface mounted laser, control and image acquisition systems during the deployments near LEO 15, May 8-20, 2000.

to continuously acquire 16 bit images at 0.5 Hz for more than 15 hours (a maximum of 13 hours was actually recorded).

We have opted to keep the laser on the boat and transmit the light to the bottom via optical fibers. The light source is a dual head, flashlamp-pumped dye laser that has a pulse-duration of 2 μs, 15 pulse pairs/s and essentially unlimited in-pair delay. This laser generates 350 mj/pulse at 594 nm, which is sufficient for pumping light through more than one fiber. Consequently, (Figure 2) we split the laser beams and focus them onto two 400 μm diameter optical fibers that transmit the light to submerged probes. The output per probe is 120 mj/pulse. This setup enables us to orient the two cameras and laser sheets *independently*, in the same or different plane, vertically or horizontally, near each other or apart. The submerged probes contain optics for generating the light sheets. The thickness of the sheet varies between 2-4 mm over the sample area. During the 2000 experiments the distance between the camera

and the light sheet was 50 cm and the field of view was 51x51 cm, requiring wide-angle lenses and a spherical dome as a front window (Nimmo-Smith et al., 2001). To calibrate the system and correct for image distortions we recorded images of a reference grid and created precision calibration maps. These calibrations were used for correcting the velocity vectors and their locations. While analyzing the data it became evident that the data was adversely affected by projection of out-of-plane motion onto to the image plane, mostly in the outer perimeter of the image. This effect was caused by the short distance between the camera and the light sheet and the relatively large thickness of the light sheet. Consequently, during the recent experiments the light sheet thickness was reduced to 2mm, the distance between the sheet and the camera was doubled and the sample area of each camera was reduced to 35x35 cm. These changes eliminated the effect of out-of plane motion.

The submersible system also contains a CTD, optical transmission and dissolved oxygen content sensors, a ParoScientific precision pressure transducer (for measuring surface waves), two biaxial clinometers (to measure the orientation of each camera) and a digital compass. An on-board vane that aligns itself to the flow and a video camera that focuses on this vane are used for indicating the flow direction. The turn-table drive then rotates the platform and aligns the laser with the mean flow. A second submerged video camera records images of the bottom topography.

Sample Results from the Deployment Near LEO

The platform was deployed at a depth of 12m in the vicinity of the LEO-15 from R/V Cape Henlopen. An on-board ADCP provided us with data on the mean velocity distribution in the water column for the duration of the tests (Figure 3). On one night we recorded data at 0.5 Hz for eight hours continuously. On the following night we recorded data at 0.5 Hz for 13 hours continuously. During these tests the cameras were configured as illustrated in Figure 1. Both focused on the same plane, and their centers were located 1m apart. The data was acquired at three elevations, 9.5-60.5 cm, 64-115 cm and 118.5-169.5 cm above the bottom. At each elevation we aligned the system to the mean flow direction and then acquired

Figure 3: ADCP data during the LEO-15 tests.

data, typically for thirty minutes, i.e. 2x1800 images. Since the flow direction changed with time and with elevation we had to re-align the platform for each data set. The extent of variability in magnitude and direction of mean current is evident from Figure 3. The numbers indicate the timing at the beginning of the 35 data series obtained during this test. Our vane direction was consistent with the ADCP data. A vector map highlighting the turbulence by subtracting the average velocity is presented in Figure 4.
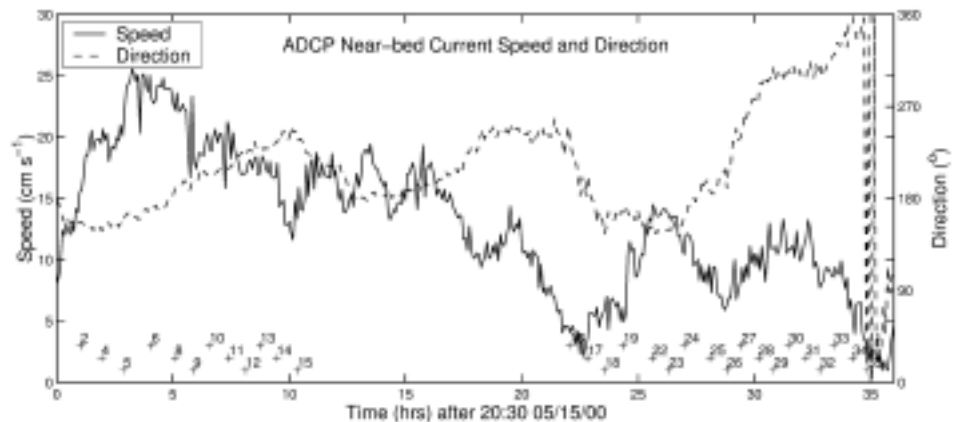
A 30 minutes example of the time evolution of the average velocity in a vector map at a given elevation is presented in Figure 5a. Each point is an average of the data over the entire vector map. The
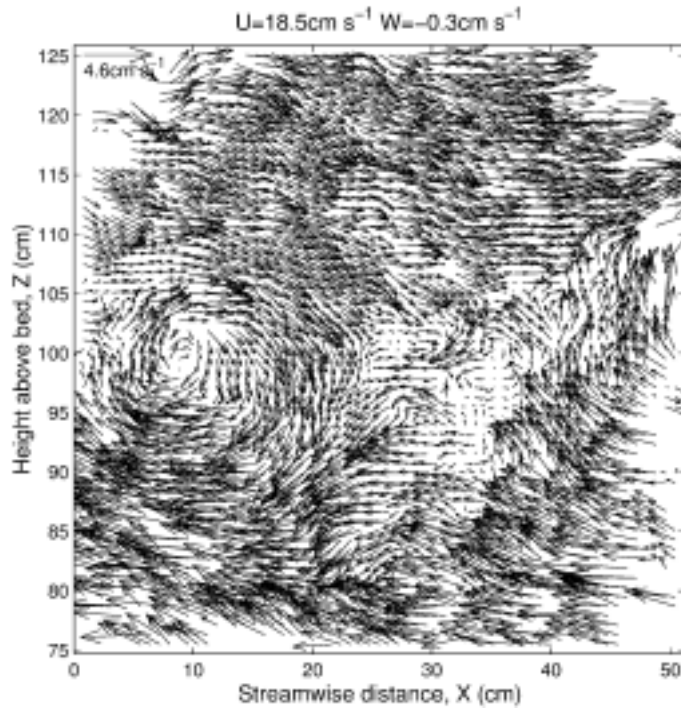
Figure 4: A vector map

effect of wave-orbital velocity and formation of wave-packets are clearly evident. We also acquired a third data set behind the wall of the harbor of refuge of the Delaware Bay.

This time the two planes were perpendicular to each other and the data was acquired at 3 Hz. This location was characterized by a stronger mean current, as shown in the five minutes sample presented in Figure 5b. We recorded five data sets at different times and elevations, each consisting of 1000 image pairs. As of today, we have analyzed al the images, obtained the velocity distributions, and corrected for distortion. Constrained by the particle concentration, we used 64x64 pixels interrogation windows and 50% overlap between windows. Thus, each vector map consists of 64x64 vectors with spacing of 0.8 cm.

In the LEO-15 data the amplitude of the wave-induced flow is comparable to the mean flow (Figure 5a). Here the mean velocity is 14 cm/s with comparable fluctuations due to surface waves. As expected, the waves have more impact on the horizontal velocity and the magnitude of the vertical velocity is low. Consistent with the ADCP data, the mean velocity varies during the tests between 10 – 20 cm/s.
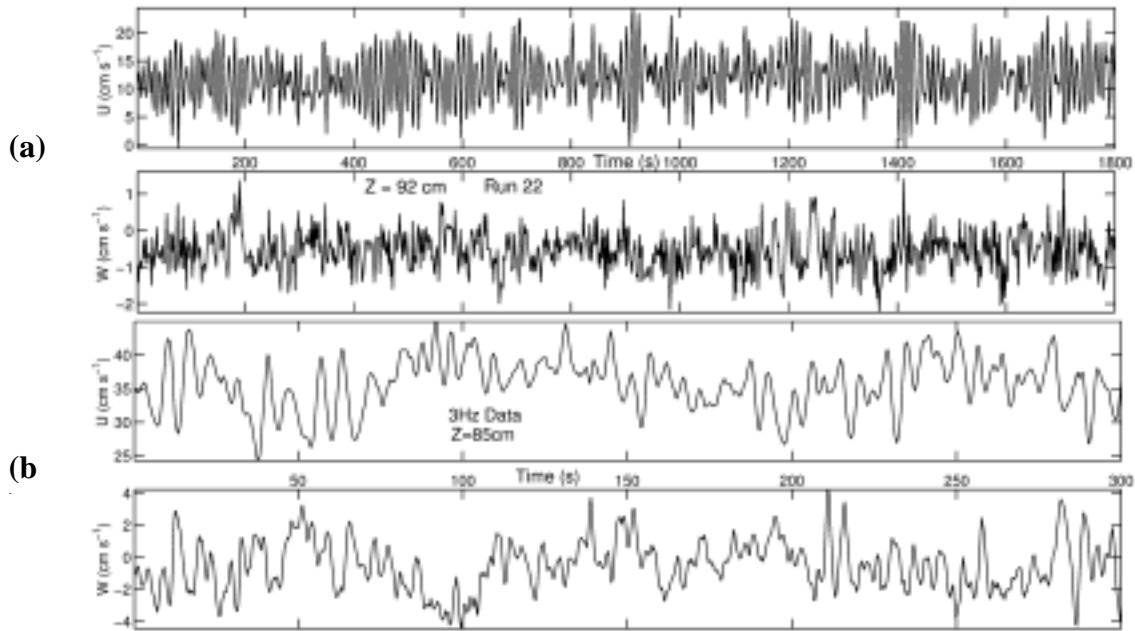
5

Figure 5: Time series of averaged velocity.
a) 0.5 Hz, LEO 15 data;
b) 3 Hz Delaware Bay data.

Under these conditions the horizontal mean velocity profiles clearly <u>do not</u> have a logarithmic profile, as illustrated in Figure 6. Conditional sampling based on the phase of the wave does not change this conclusion. Conversely, when the mean flow is substantially faster than the wave-induced motion, such as the conditions shown in Figure 5b, a log layer does forms (Figure 7). A log layer forms only when the mean flow is substantially faster than the orbital motion.
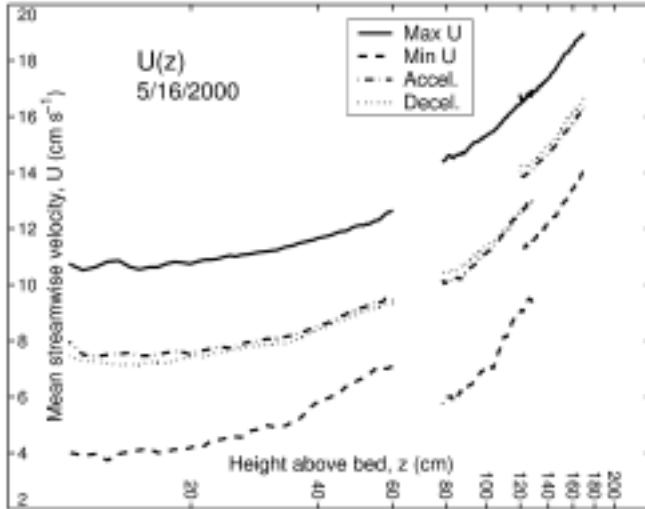

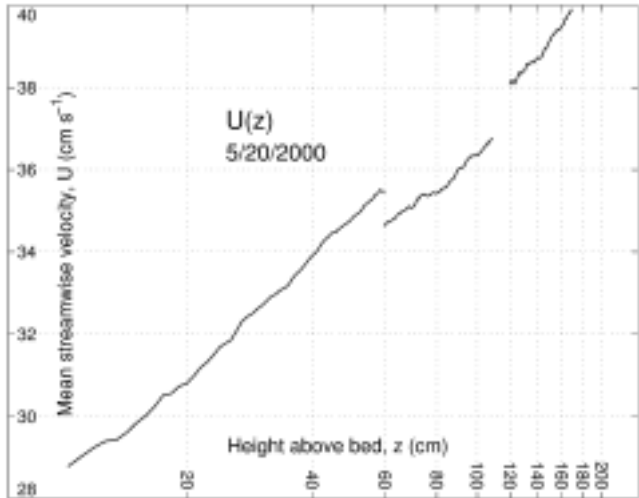*Figure 6: Conditionally sampled distributions of U(z) at different phases of the wave motion. LEO 15 data.*

Figure 7: Distributions of U(z). Delaware Bay 15 data.

Measurements of Reynolds Stresses

To calculate the Reynolds shear stresses and overcome the problems introduced by waves we follow (1998), modifying his procedure to take advantage of the 2-D velocity distribution provided by PIV. If the velocity can be decomposed to $u_i = \overline{u}_i + u_i^w + u'_i$, where overbar is the time average, u_i^w is wave induced motion and u'_i is the turbulence contribution. Defining $\Delta u_i = u_i(x_i + r_i) - u_i(x_i)$, then

$$\text{cov}[\Delta u_i, \Delta u_j](r_i) = \overline{[u_i(x_i + r_i) - u_i(x_i)][u_j(x_i + r_i) - u_j(x_i)]}$$

Assuming horizontal homogeneity, no correlation between u_i^w and u'_i, and that the integral scale, l, is much smaller than the wavelength of surface waves, one obtains:

$$\text{cov}[\Delta u_i, \Delta u_j](r_i) = 2\overline{[u'_i u'_j]} - 2\overline{[u'_i(x_i + r_i)u'_j(x_i)]}$$

The first term on the right hand side is (twice) the Reynolds stress and the second term is the structure function, $R_{ij}(r_i)$. Typically $R_{ij}(r_i)$ decreases with increasing r and diminishes for r is larger than the integral scale. Thus, for $l < r << \lambda$, $\text{cov}[\Delta u_i, \Delta u_j](r_i) \approx 2\overline{[u'_i u'_j]}$, i.e. the stress is equal half of the covariance of the velocity differences. Trowbridge (1998) shows that this method substantially reduces the wave contamination due to instrument alignment. Using the PIV data and assuming horizontal homogeneity one can calculate $\text{cov}[\Delta u, \Delta w](r_1)$ using data obtained in a vertical plane and $\text{cov}[\Delta u, \Delta v](r_1)$ using the horizontal sheet data. The two 51x51 cm samples aligned horizontally in the same plane with a gap of 50 cm between them enable us to calculate $\text{cov}[\Delta u, \Delta w]$ up to a scale of $r_1 = 1.5$m by directly multiplying the appropriate velocity components. Up to 51 cm the two vectors are located in the same map and for larger scales one vector comes from each map. Assuming horizontal homogeneity one can average data obtained at different x (but the same z) as well as at different times. A sample distribution of $\text{cov}[\Delta u, \Delta w]$ is presented in Figure 8. Initially the values of $\text{cov}[\Delta u, \Delta w]$ increase with r_1, and then they asymptotically converge to a constant value as r_1 becomes comparable to the distance from the bottom. The condition of $r << \lambda$ is also satisfied ($\lambda = 100$ m). Thus, the expected trends indeed occur and $\overline{u'w'} = 0.2$ cm^2/s^2. Sample distributions of $\text{cov}[\Delta u, \Delta v]$ and $\text{cov}[\Delta u, \Delta w]$ obtained using data recorded with perpendicular planes are presented in Figure 9. Here the range of r_1 is limited to one sample area, but the results start reaching asymptotic values. Thus, $\overline{u'w'} = 0.3$ cm^2/s^2 and $\overline{u'v'} = 0.05$ cm^2/s^2.
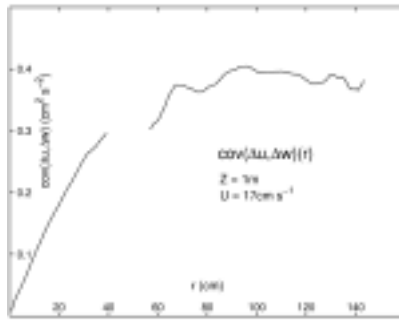

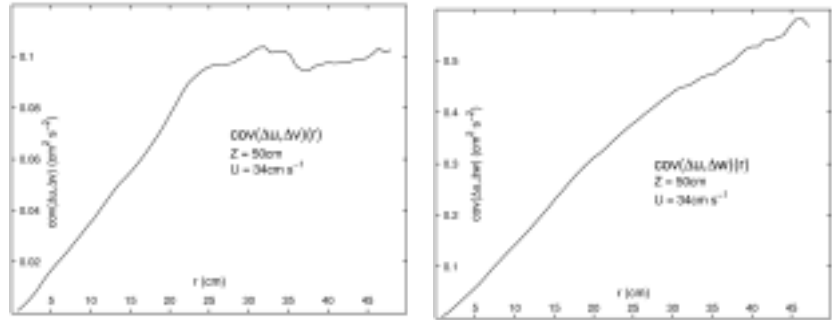*Figure 8:* $\text{cov}[\Delta u, \Delta w]$ *using data of two vector maps (Figure 7). LEO-15.*

Figure 9: $\text{cov}[\Delta u, \Delta w](r_1)$ *(right) using data obtained in a vertical plane and* $\text{cov}[\Delta u, \Delta v](r_1)$ *(left) using a horizontal sheet data. Delaware Bay.*

Field Tests during 2001 and The Large Profiling Platform.

Consistent with the objectives the NSF funded project to extend the profiling range to the water column, we have also constructed and tested a new platform that extends our profiling capability up to 9.75 m above the bottom. The system is shown in Figures 10a and b. This platform consists of a hydraulic telescopic arm with five elements. When fully retracted, the entire system elevation is 2.6 m and when fully extended it is 12.35 m long. Thus, it can be transported and deployed, but provides a substantial profiling range. To insure stability the tube diameters range from 28 cm to 13 cm with a

EXTENDED

Camera (x2)

Light Sheet (x2)

Smallest Moving Stage: 13cm Dia.

Extension Range: 9.75m

5-Stage Double-Acting Telescopic Hydraulic Cylinder

Largest Moving Stage: 25cm Dia.

Turntable

RETRACTED

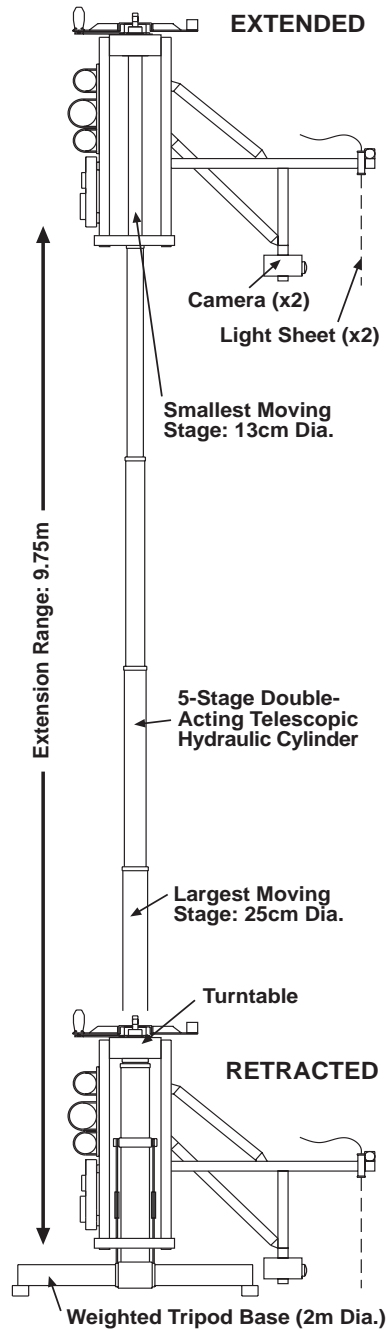**Weighted Tripod Base (2m Dia.)**

Figure 10: (a -left) the new platform in retracted and extended configurations; (b - right) The platform partially extended.

wall thickness is 0.635 cm. The system weight is 1180 Kg (with the instrumentation), but the weight is increased to 2700 Kg by adding lead bricks at the bottom legs. The instruments are installed on a turntable driven by a hydraulic motor and attached to the top of the platform.

The optical fibers, optics, cameras, image acquisition systems and other instruments are the same as those used in the previous deployment (Figures 1 & 2). During the recent deployments on September, 2001, we have also installed a turbulence measurement package containing airfoil probes. This instrument provides a time series of data on the out of plane velocity component at the same elevation but at a different location (to minimize the disturbance to the flow). The system also includes a video camera equipped with a microscope objective for continuous monitoring of the characteristics of the particles in the sample area. A strobe light with an optical fiber delivery system is used for illumination.

Deployments tests of the new platform took place during May 18-26, 2001. Experiments to acquire data took place September 1-10, 2001. We successfully obtained a substantial data series within the boundary layer (ONR project) and in the water column above it. Included are PIV images recorded at 1 - 3.33 Hz for 20 minutes at each elevation near the bottom and at elevations of 1, 2, 4, 6 and 8m. Overall we recorded 88,800 images (700GB). Analysis to obtain the velocity distributions is in progress. For the entire duration of the tests we also have CTD data, mean currents distributions (using ship ADCP), a complete record of airfoil probes data, and video records at high magnifications for measuring the particle distributions. We expect to complete the process of calculating the velocity distributions in the next two months.

IMPACT

The present measurements provide us with an opportunity to address issues related to flow structure and turbulence in the bottom boundary layer of the coastal ocean. Included are distributions of Reynolds stresses, spectra, turbulence production and dissipation, all free of contamination by surface waves. We can also determine the effects of large scale forcing on these parameters, study the dynamics of large-scale coherent structures and their effect on sediment entrainment, and address fundamental questions related to applications of Large Eddy Simulations to oceanic flow modeling.

TRANSITIONS

During FY 2000 & 2001 the submersible PIV system has been used extensively at NSWC/Carderock to measure the flow structure within wakes behind several maneuvering models.

RELATED PROJECTS

The research involving measurements of flow structure and turbulence in the coastal ocean using PIV has been funded in part by ONR (present project) and in part by NSF (9871961). The NSF sponsored project focuses with the flow/turbulence in the water column above the boundary layer, whereas the present project focuses on the boundary layer.

REFERENCES

Bertuccioli, L., Roth, G.I., Katz, J., Osborn, T.R. (1999) "Turbulence measurements in the bottom boundary layer using particle image Velocimetry," *J. Atmos. Oceanic Technol.*, **16**, 1635-1646.

Doron, P., Bertuccioli, L., Katz, J., Osborn, T.R., (2001), "Turbulence Characteristics and Dissipation Estimates in The Coastal Ocean Bottom boundary Layer from PIV Data," *J. Physical Oceanography*, **31**, 8, 1, 2108-2134.

Trowbridge, J.H., (1998), "On a technique for measurement of turbulent shear stress in the presence of surface waves*," J. Atmos. Oceanic Technol.*, **15**, 290-298.

PUBLICATIONS

Doron, P., Bertuccioli, L., Katz, J., Osborn, T.R., (2001), "Turbulence Characteristics and Dissipation Estimates in The Coastal Ocean Bottom boundary Layer from PIV Data," *J. Physical Oceanography*, **31**, 8, 1, 2108-2134.

Nimmo Smith, W.A.M., Atsavaprani, P., Zhu, W., Luznik, L., Katz, J., Osborn, T.R., (2001), "PIV Measurements in the Bottom Boundary Layer of the Coastal Ocean," 4th International Symposium on Particle Image Velocimetry, Göttingen, Germany, September 17-19.